

Synthesis and Characterization of Hydrophilic Nanocomposite Coating on Glass Substrate

Azam Rahimi, Salimeh Gharazi, Amir Ershad-Langroudi, Diba Ghasemi

Department of Polymer Science, Iran Polymer and Petrochemical Institute, Tehran, Iran

Received 16 January 2006; accepted 26 May 2006

DOI 10.1002/app.24884

Published online in Wiley InterScience (www.interscience.wiley.com).

ABSTRACT: Hydrophilic coatings based on 3-glycidoxy propyl trimethoxy silane (GPTMS) and polyethylene glycol (PEG) were prepared with the incorporation of tetramethoxysilane (TMOS) and silica nanoparticle colloidal suspension by a sol-gel process. Characterization of the coatings has been performed by Fourier Transform Infrared (FTIR) and Attenuated Total Reflectance Infrared (ATR-IR) techniques. Morphological properties were characterized by Scanning Electron Microscopy (SEM). The distribution of Si atoms in the hybrid system was obtained by Si mapping. The particle size in sol solution of the coating was measured by light scattering analyzer. Optical properties were characterized by using UV-vis spectrophotometer.

The hydrophilicity of the coating was determined by contact angle measurements, and also the results have been confirmed by surface energy and water uptake investigations. The obtained results indicate that the surfactants affected the contact angles remarkably but did not change the transparency. It has been found that applying silica nano particles leads to coatings with different properties than those using TMOS, while siloxane contents were the same in these two set of coatings. © 2006 Wiley Periodicals, Inc. *J Appl Polym Sci* 102: 5322–5329, 2006

Key words: synthesis; hydrophile; coating; nanocomposite; glass

INTRODUCTION

Glass is a kind of material which is used in buildings, vehicles, airplanes, trains, and display screens in a variety of other applications because of its transparency combined with complete impermeability to gases and liquids. However, for an increasing several important applications, additional properties are required, for example, control of light transmission in a passive or even active way or control of surface chemistry in response to environmental factors (moisture and dust).

Fogging on glass surfaces is an undesirable effect most of the time. It is due to water droplet condensation when the temperature goes below the dew point.^{1,2} Several investigations have been conducted to produce antifogging coatings.^{1–7} Most of them have only a temporary antifogging effect, because they are liquid mixture or water proof materials, which are simply applied on the substrate surfaces. Thus, it is necessary to produce a new coating material with good adhesion properties which can enhance the antifogging effect. Sol-gel process is known as a convenient process for preparing designed material for coat-

ing.^{6–9} Hydrophilic coating sol-gel solutions were prepared using (3-Glycidoxypropyl)trimethoxysilane (GPTMS) and silica suspension.^{1–7} Yu and coworkers reported the preparation and characterization of porous TiO₂ coating films.⁵ Schmidt et al. have reported antifogging coating using epoxysilane.^{1,2,10} In the present work we prepared transparent nanocomposite coating films via the sol-gel method on glass and it was characterized by Fourier Transform Infrared (FTIR), Scanning Electron Microscopy (SEM), and light scattering techniques. The water contact angle of coating films was also tested and the effect of surface microstructure on them was discussed.

EXPERIMENTAL

Materials and reagents

(3-Glycidoxypropyl)trimethoxysilane (GPTMS), tetramethoxysilane (TMOS), and 1-methylimidazol were purchased from Fluka (Dubai). Polyethylene glycol (PEG) with average molecular weight of 200 designated as PEG200 was purchased from Merck (Tehran, Iran) and used as received. A commercial silica suspension (Ludox-LS, Aldrich, Dubai) was used to prepare coating solution. Ludox-LS consisted of 30% silica colloidal particles (12 nm average diameters) and 70% water. Hydrogen chloride was purchased from Merck and used without further purifi-

Correspondence to: A. Rahimi (a.rahimi@ippi.ac.ir).

TABLE I
Chemical Components of the Samples

| Sample ^a | PEG (wt %) | Surfactant (wt %) | TMOS (wt %) | Silica suspension (wt %) |
|---------------------|------------|-------------------|-------------|--------------------------|
| A | 0 | 0 | 0 | 0 |
| B | 30 | 0 | 0 | 0 |
| C | 30 | 1 | 0 | 0 |
| D | 30 | 0 | 11 | 0 |
| E | 30 | 0 | 0 | 30 |

^a SiO₂/H₂O in all samples is 100% stoichiometric, Methylimidazole/GPTMS is 1/1, and GPTMS is 50%.

cation, and polyoxyethylene louril ether (Brij 30) purchased from Aldrich.

Sol preparation

The hybrid sol was prepared by admixing SiO₂ (GPTMS and TMOS) precursors and PEG200 as follows:

SiO₂ was placed in a beaker with stoichiometric molar ratio of water and vigorously stirred with magnetic stirrer for 1 h at room temperature. Then PEG200 was added to the solution and stirred again for 3 h at ambient conditions. Before coating, 1-methylimidazol was added under stirring for 1 h. After having been stirred with surfactant for 10 min, the transparent sol applied onto substrate surfaces by standard dip coating methods. Table I represents chemical compositions of the sample.

Substrate preparation

Slide soda glass plates of size 25.4 × 76.2 × 1.2 mm³ were used as the support substrate. They were carefully cleaned by methanol and dried in air.

Characterization

Attenuated total reflectance infrared spectroscopy (ATR-IR) was used for chemical surface analysis. Infrared spectra were recorded using ATR objective of a bruker IFS 484 microscope between 400 and 4000 cm⁻¹. Additionally to characterize the surface morphology of the coated substrate Scanning electron microscopy technique (SEM) was performed with a Cambridge S360 microscope using a back scattered or a secondary electron image detector at 20 KV and 2.85 A probe current. The distribution of Si atoms in the hybrid system was obtained by SEM EDX mapping (LEO 440) in which Si atoms were denoted by white points. Using light scattering analyzer, SEMATech 39 chem du Terron 06,200 NICE-

France, the particle size in the coating solution was measured. Optical characterizations were determined by using a UV-vis spectrophotometer (Type UV: CECIL 1021, wave length range 200–800 nm).

Contact angle

The hydrophilic property of coating films was studied by measuring the contact angle of water on various films. The advancing contact angle for water was measured by the extension method with a horizontal protractor eyepiece at room temperature (type: contact angle measuring system G10 KRUS) and used as contact angles. Water droplets were placed at five different positions for one sample and the averaged value was adopted as the contact angle. To ensure repeatability, the size of attached water droplets was always kept constant which was about 5 μL after 1 min at each test. Also the surface free energy was studied using Owens and Wu methods.^{11,12}

Water uptake

The samples with finite primary weight (W_g) were immersed in distilled water at 25°C for 4 h. Surfaces of wet films immediately weighed and secondary weight (W_s) was obtained. The films water uptake (WR) was measured by this equation^{13,14}:

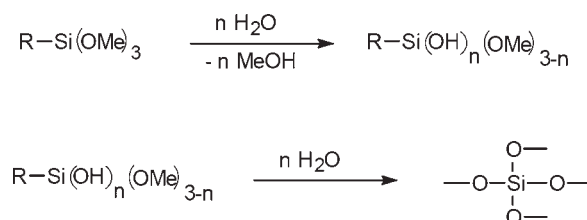
$$WR\% = \frac{W_s - W_g}{W_g} \times 100$$

RESULTS AND DISCUSSION

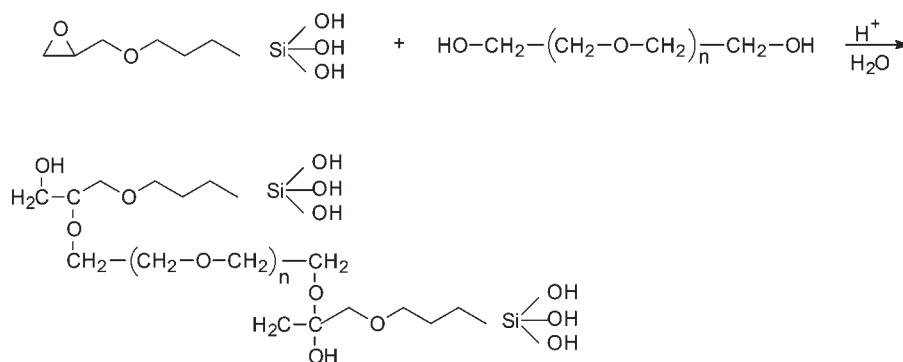
The hydrolysis and condensation reaction of the alkoxy silane precursor is catalyzed by hydrochloric acid (Scheme 1).

The major portion of hydrolyzed GPTMS reacts with polyethylene glycol reagent and covalent bonds are formed upon epoxy ring opening. The mechanism of the reaction is proposed in Scheme 2.

In addition, methylimidazole agent reacts with GPTMS and completes the epoxy ring opening and also catalyzes crosslinking reaction of Si—O and



Scheme 1 Hydrolysis and condensation of the alkoxy silane.



Scheme 2 Reaction of PEG with GPTMS.

C—O groups and the C—O—Si and Si—O—Si bonds formation (Scheme 3).

FTIR analysis

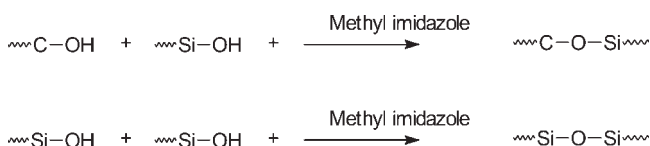
The IR spectrum of the sol solution (containing GPTMS and H₂O at pH = 2) after 1 h hydrolysis is shown in Figure 1(a): Stretching vibration band of ether group appears in the region 1050–1150 cm⁻¹, with maximum peak at $\nu = 1100$ cm⁻¹, characteristic alkyl (R—CH₂) stretching modes observed at $\nu = 2850$ –3000 cm⁻¹, hydroxyl group vibration band appears at $\nu = 3200$ –3500 cm⁻¹, and also the absorption bands of epoxy group at $\nu_{\text{as}}(\text{CH}_2) = 3003$ cm⁻¹, $\nu_{\text{b}}(\text{CH}_2) = 1479$ cm⁻¹, $\nu(\text{C—O}) = 1255, 908, \text{ and } 850$ cm⁻¹.

The appearance of methylene group vibration band at 2990 cm⁻¹ in IR spectra of sol solution after addition of PEG indicates the epoxy ring opening [Fig. 1(b)], as mentioned earlier methylene group attached to epoxy ring absorbs at 3003 cm⁻¹.¹⁵

The ATR-IR spectra of coating films on glass before and after adding PEG₂₀₀ are shown in Figure 2(a,b), respectively. The epoxy ring absorption bands appear at 906 and 758 cm⁻¹ with its intensity decreasing due to epoxy ring opening [Fig. 2(b)].

With the addition of methyl imidazole to the reaction mixture, crosslinking reaction and epoxy ring opening are completed and the formation of the C—O—Si and Si—O—Si bonds are confirmed by appearance of their absorption bands at 1107, 831, and 1098 cm⁻¹, respectively, [Figs. 1(c) and 2(c)].

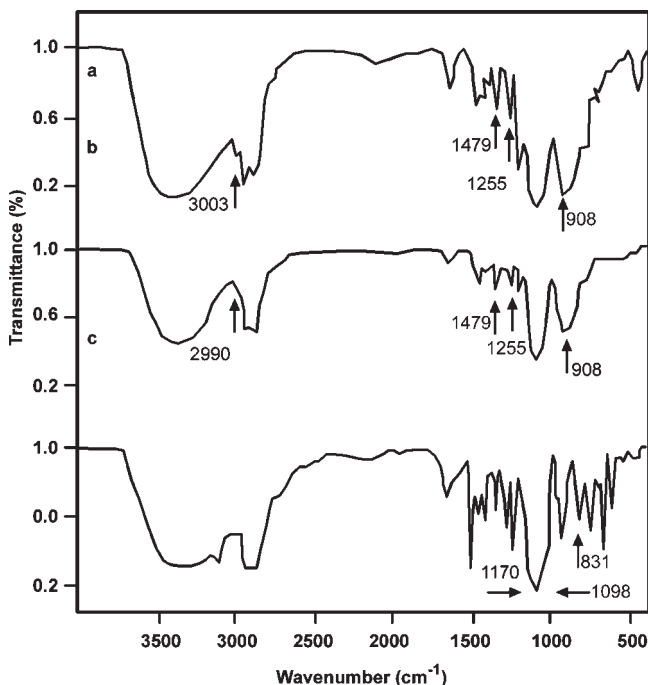
Also, the absorption band at 1650 cm⁻¹ in Figure 1(c) is related to H₂O bending vibration which confirms the occurrence of condensation reaction.



Scheme 3 Crosslinking reaction with methyl imidazole.

Morphological investigations

Light scattering technique was employed to study the sol solution. The results show that the size of majority of particles is about 4 nm. Therefore, it can be concluded that no agglomeration of particles as occurred in the sol solution. Moreover, for particle size investigation, on the coating after curing by heat treatment, Si mapping and SEM techniques have been employed. The distribution of Si atoms in the hybrid system was characterized by SEM EDX mapping (LEO 440) in which Si atoms were denoted by white points. Figure 3 represents Si mapping of the hybrid nanocomposite sample A. As seen from this image, these silica particles (white points) have uniform distribution and they are more condensed in the glass substrate (a) than the hybrid coating (b).

Figure 1 FTIR spectra of sol solution after: 1 h hydrolysis (a), PEG₂₀₀ addition (b), and methyl imidazole addition (c).

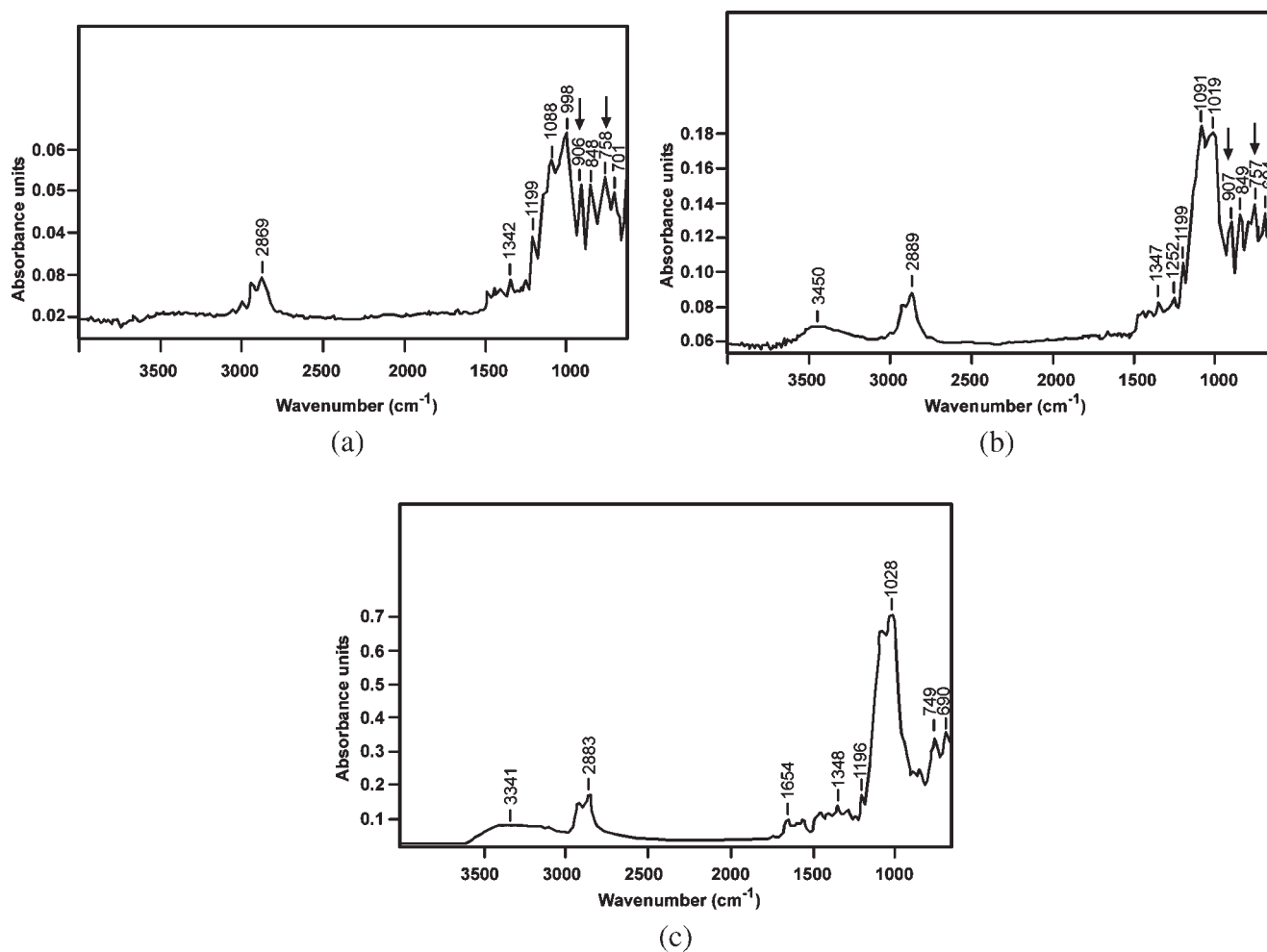


Figure 2 ATR-IR spectra of the coating on glass after: (a) 1 h hydrolysis of GPTMS (b) PEG₂₀₀ addition, and (c) methylimidazol addition.

The morphology of the coating surface was also elucidated by SEM micrograph of the coated substrate to characterize the surface morphology. Figure 4,

shows SEM micrograph of the surface area of the sample A. In addition, similar results are obtained on the other samples. These observations may be

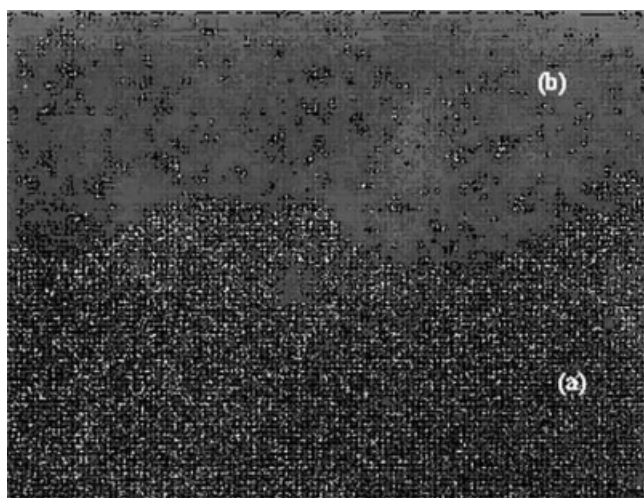


Figure 3 Si mapping of hybrid nanocomposite.

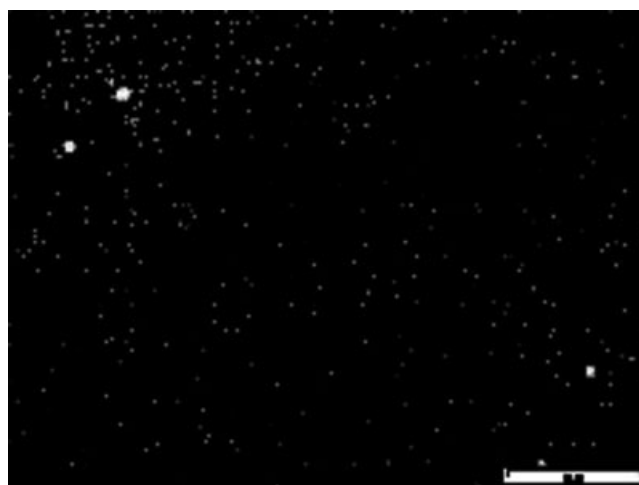


Figure 4 SEM micrograph of sample A.

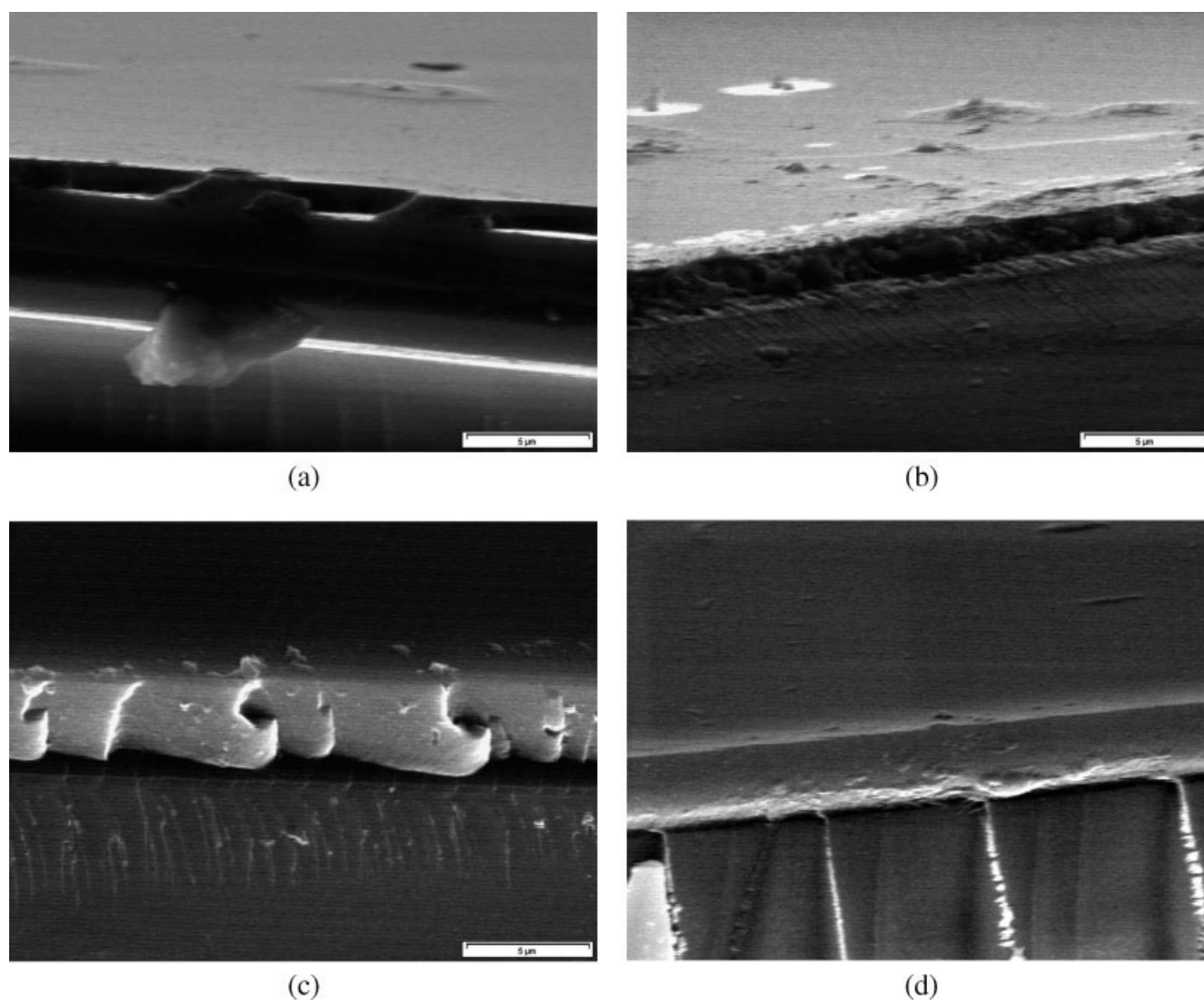


Figure 5 SEM micrographs of (a) sample A, (b) sample B, (c) sample E, (d) sample D.

attributed to the fact that complete interpenetration of the organic and inorganic phases occurred and no aggregation in the coating solution and on the coated substrate observed. We were led to this assumption that the samples contain organic and inorganic phases at the molecular level. Therefore, it can be concluded that these hybrid coating films are molecular composites due to the molecular scale of their morphology.¹⁶ However, different microstructure were developed in coating films prepared from precursor solutions with organic and inorganic

reagents such as PEG, TMOS, and silica suspension. It is observed that coating films prepared from the precursor solution without PEG [Fig. 5(a)] has flat texture (sample A). By comparing the Figure 5(a,b) it can be concluded that the addition of PEG to hybrid coating films transforms the surface morphology from flat texture to rough surface to some extent. In addition SEM micrograph of sample A and sample B indicates a good adhesion between coating and glass substrate that may be due to the formation of Si—O—Si bond between hybrid coating and glass

TABLE II
Relationship Between Samples and Thickness (μm)

| Sample | Thickness |
|--------|-----------|
| D | 2.87 |
| E | 3.17 |

TABLE III
Transmittance of Samples Using UV-Vis Spectra

| Sample | Transmittance |
|--------------------|---------------|
| Glass (no coating) | 90 |
| A | 89 |
| B | 88 |
| C | 87 |

TABLE IV
Water Contact Angles of the Samples

| Sample | Contact angle |
|--------|---------------|
| A | 64 |
| B | 42.3 |
| C | 5.4 |
| D | 41.2 |
| E | 39.8 |

substrate which was also supported by ATR-IR results.

According to Figure 5(c), it is observed that silica suspension incorporated in the hybrid sol improved the adhesion between coating and glass substrate, but incorporation of TMOS in the sol [Fig. 5(d)] led to lower adhesion which is due to less contribution of organic part in stress support of samples. As, Hajji et al.¹⁷ have found that silica particles in the sol tend to form aggregates in the continuous phase, while *in situ* synthesizing of the inorganic network by TMOS results in a much finer morphology and more complete bi-continuous polymer-silica network. Therefore, molecular mobility in the silica suspension system is more increased than the other system which contains TMOS in its network. Thus it lowers the flexibility of the coatings which leads to lower adhesion.

As it was mentioned, *in situ* polymerization with TMOS causes finer microstructure in comparison with applying silica suspension (sample E), which indirectly exhibited with thickness measurement by SEM as seen in Table II.

UV-vis studies

Visible light (380–780 nm) transmittance of the coating films was studied by UV spectroscopy technique and data are shown in Table III. Good transparency of these coatings is due to matching of the refractive index of coating layer and the glass substrate.³

According to Table III, all the samples show good transparency. It can be described by the fact that the miscibilities of the PEG, GPTMS, and surfactant are so good that the migration of surfactant to the surface is not enough to affect the transparency of the coatings.

TABLE V
Surface Free Energies (mN/m) of Liquid Used for Contact Angle Measurements^{11,12}

| Liquid | γ_1 | γ_1^d | γ_1^p |
|-----------|------------|--------------|--------------|
| Water | 72.8 | 18.7 | 53.6 |
| Formamide | 59 | 39.4 | 19.6 |
| Glycerin | 65.2 | 39.4 | 19.6 |

TABLE VI
The Results of Interfacial Energy and Critical Interfacial Energy Obtained by Owens-Wendt-Rable and Kaebler

| Sample | γ | γ^p | γ^d |
|--------|----------|------------|------------|
| A | 37.9 | 20.6 | 17.3 |
| B | 52.9 | 35.5 | 17.4 |
| C | 75.7 | 71.6 | 4.1 |
| D | 54.8 | 37.4 | 17.4 |
| E | 58.7 | 36.9 | 16.8 |

Contact angle measurements

It is well known that the wetting behavior of solid surfaces depends on their surface chemistry.³ The hydrophilic property of the coating was confirmed by water contact angle measurements. Table IV shows the water contact angles of the coatings. The water contact angles obtained are in the range of 5–64°. The silica coating films prepared from the precursor solution containing PEG200 (samples B, D and E) have lower contact angle compared to sample A. It may be related to the more COH groups of the samples containing PEG200 resulted from epoxy ring opening during the reaction. Thus, high concentrations of nonionic hydrophilic COH groups can decrease hydrophobic component adsorption.^{1,2} The increase in hydrophilicity is mainly due to existence of C—O polar groups in these samples (B, D, and E) which was shown by surface tension measurements. It is found from Table IV that sample C had the lowest contact angle in comparison with the other samples. It is due to the fact that incorporation of surfactant in sample C increases the hydrophilicity of the coating by thermodynamically controlled enrichment of the surface by hydrophile end groups.¹⁸

To get more information on the surface energy of the hydrophilic coating, the contact angle measurements were carried out by using probe liquids (Tables IV–6) other than water. To determine the polar (γ_1^p) and dispersive components of the surface tension we used Owens and Wu equations. According to Tables V–VII γ_1^p did not change by the addition of Silica and TMOS to the coating solution (sample B). Infact, samples D and E have the same silane content, in spite of morphological changes

TABLE VII
The Results of Interfacial Energy and Critical Interfacial Energy Obtained by Wu Method

| Sample | γ | γ^p | γ^d |
|--------|----------|------------|------------|
| A | 40.9 | 32.6 | 8.3 |
| B | 57.8 | 49.7 | 8.2 |
| C | 89.6 | 85.9 | 3.7 |
| D | 59.9 | 49.9 | 9.1 |
| E | 58.4 | 49.8 | 8.5 |

[SEM micrographics in Fig. 5(c,d)], the surface tensions of the both samples are the same, which may be attributed to the fact that morphological properties have not influenced intensively by the distribution of inorganic phase.

According to Tables IV–VI, the addition of surfactant in sample C had a remarkable influence on the wetting behavior even though γ_1^p is higher than γ_1^p of water. One possible explanation is that the incorporation of hydrophilic components (nonionic surfactant) caused the controlled release of surfactant to the surface. The released surfactant can decrease the interfacial tension of condensed water which leads to film condensation.^{1,2,8}

One can conclude that the polar fraction of surface tension is increased by applying the hybrid sol on the glass substrate in the presence of nonionic hydrophilic surfactant.

Effect of pH on contact angle

As pH was increased, contact angles were changed as follows:

| pH | Contact angle |
|----|---------------|
| 2 | 0 |
| 4 | 30 |
| 7 | 32 |
| 10 | 0 |

It can be seen that contact angles of the coatings prepared at pH = 2 and 10 were lower than contact angles of those prepared at pH = 4 and 7. Because at pH = 2 and 10 (i.e., in acidic or basic conditions) the hydrolysis and condensation reactions are almost completed. The coatings prepared at pH = 2 are more uniform than those prepared at pH = 10, due to linear structure of the network, instead of cluster formation that occurred at pH = 10.¹⁹

Water uptake

Water uptake values were determined for the sample series in Table VIII then, the coatings were kept at 100°C for 30 min and their contact angles were measured.

TABLE VIII
Water Uptake and Contact Angles of the Samples

| Sample | Water uptake | Contact angle |
|--------|--------------|---------------|
| A | 3.74 | 67 |
| B | 4.15 | 42 |
| D | 4.95 | 42 |

Increasing water uptake values for sample B in comparison with sample A indicates more hydrophilicity of the PEG component in the hybrid coating. Silica incorporation in these reactions resulted in more roughness and particularly more sites for water absorption on the coating surface even physically. Nevertheless, measuring contact angle after water uptake experiments indicates that almost in these samples the contact angle is constant which is due to more strong bond formation in the samples.

CONCLUSIONS

It is found that the hybrid organic–inorganic samples retains their structure in molecular level even after curing. This assumption is studied by light scattering, Si mapping, and SEM imaging techniques. In addition good adhesion between coating and glass substrate were observed in coated samples that were due to the formation of Si–O–Si bond between hybrid coating and glass substrate. It was also supported by ATR-IR analysis. Good transparency of these coatings is due to well matching of the refractive indexes of the coating layer and the glass substrate which was investigated by UV–vis analysis. The experimental results show that hybrid systems containing PEG can be successfully developed to produce thin film at room temperature. Hydrophilic PEG200 chains can be introduced in the hybrid system, leading to an improvement in the wetting behavior without losing transparency. However, the addition of surfactant had a remarkable influence on the wetting behavior even though the polar components of some samples were higher than that of water. It was confirmed by interfacial energy measurements and contact angle studies.

The authors express their sincere gratitude to Miss. Soraya Mir Mohammad Sadeghi (editor of Iranian Polymer Journal) for careful editing of the manuscripts.

References

- Schmidt, H. *J Non-Cryst Solids* 1994, 178, 320.
- Kasmann, R.; Schmidt, H. Presented at the First European Workshop on Hybrid Organic-Inorganic Materials, France, November 8–10, 1993.
- Song, K.; Park, J.; Kang, H.; Kim, S. *J Sol-Gel Sci Technol* 2003, 27, 53.
- Kron, J.; Aamberg-Schowab, S.; Schotner, G. *J Sol-Gel Sci Technol* 1994, 2, 189.
- Yu, J.; Zhao, X.; Zhao, Q.; Wang, G. *Mater Chem Phys* 2001, 68, 253.
- Meincken, M.; Roux, S. P.; Jacobs, E. P. *Appl Surf Sci* 2005, 252, 1772.
- Schmidt, H. *Macromol Symp* 2000, 159, 43.
- Schottner, G. *Chem Mater* 2001, 13, 3422.
- Kasmann, R.; Schmid, H. *J Chem* 1994, 18, 1117.

10. Kasmann, R.; Schmid, H.; Arpac, E.; Gerhard, V.; Geiter, E.; Wanger, G. U.S. Pat. 6,228,921 B1, 1999.
11. Wu, S. *Polymer Interface and Adhesion*; Marcel Dekker: New-York, 1982.
12. Owens, D. K.; Wendt, R. C. *J Appl Polym Sci* 1996, 13, 1741.
13. Torbati, M. A.; Saadatabadi, A. R.; Abdekhodaei, M. J. Presented at the 7th National Iranian Chemical Engineering Congress, Tehran, Iran, October 28–31, 2002.
14. Cuming, W.; Tongwen, X.; Ming, G.; Weihua, Y. *J Membr Sci* 2005, 24, 111.
15. Silverstein, R. M.; Webster, F. X. *Spectrometric Identification of Organic Compounds*; Wiley: New York, 1916.
16. Park, J. Y.; Acar, M. H.; Akhakul, A.; Kuhlman, W.; Mayes, A. M. *Biomaterials* 2006, 27, 85.
17. Hajji, P.; David, L.; General, J. F.; Pascault, J. P.; Vigier, G. *J Polym Sci Part B: Polym Phys* 1999, 37, 3172.
18. Shmidt, K. H.; Schneider, H.; Mennig, M. Presented at the 7th International Conference on Nanostructured Materials, Germany June 20–24, 2004.
19. www.psrc.usm.edu/mauritz/sol-gel.html.